Optimization of Constraint Location, Orientation, and Quantity in Mechanical Assembly

Leonard Rusli
e-mail: rusli.10@osu.edu

Anthony Luscher
e-mail: luscher.3@osu.edu

Department of Mechanical and Aerospace Engineering,
The Ohio State University,
201 W 19th Avenue,
Columbus, OH 43210

James Schmiedeler
Department of Aerospace and Mechanical Engineering,
University of Notre Dame,
257 Fitzpatrick Hall,
Notre Dame, IN 46556
e-mail: schmiedeler.4@nd.edu

A mechanical assembly aims to remove 6 degree-of-freedom (DOF) motion between two or more parts using features such as fasteners, integral attachments, and mating surfaces, all of which act as constraints. The locations, orientations, and quantity of these constraints directly influence the effectiveness of a constraint configuration to eliminate DOF; therefore, constraint design decisions are crucial to the performance of a mechanical assembly. The design tool presented in this paper uses an analysis tool developed by the authors to explore a user-specified constraint design space and help the designer make informed decisions based on quantitative data so as to optimize constraint locations and orientations. The utility of the design tool is demonstrated with an assembly case study that contains both threaded fasteners and integral attachments. The results identify the opportunity for significant improvements by separately exploring individual design spaces associated with some constraints and further gains through a search of a multidimensional design space that leverages interaction effects between the location and orientation variables. The example also highlights how the tool can help identify nonintuitive solutions such as nonrectilinear, nonplanar parting lines. A trade-off study demonstrates how the design tool can quantitatively aid in optimizing the total number of constraints. Adding constraints generally improves an assembly's performance at the expense of increased redundancy, which can cause locked-in stresses and assembly inaccuracies, so the design tools helps identify new/removable constraints that offer the greatest/least contribution to the overall part constraint configuration. Through these capabilities, this design tool provides useful data to optimize and understand mechanical assembly performance variables. [DOI: 10.1115/1.4024314]

1 Introduction

From a kinematic and structural point of view, assembly is the removal of DOF and the transfer of loads between bodies. For plastic parts, this DOF removal is typically accomplished through combinations of mating surfaces, threaded fasteners, and snap-fits without reliance on friction [1]. Extra assembly features are often included to create a highly redundant assembly because a designer lacks knowledge of the effectiveness and/or load sharing capability of the individual fastening features. Constraint redundancy offers greater resistance to undesired motions within the assembly, but it makes the parts subject to locked-in stresses due to manufacturing variations.

An optimal assembly design removes all DOFs and maximizes part constraining strength, while minimizing the number of required fastening features and placing them in their most effective locations and orientations. This design task, however, is rarely approached in a systematic or scientific manner due to a lack of formal evaluation tools for optimizing constraint strength. For example, the decision of where to divide a 3D structure into an assembly of individual components is critical in terms of both minimizing manufacturing cost and maximizing constraint, yet parting lines are traditionally formed along a single cutting plane and joined by a number of threaded fasteners that are heuristically deemed effective. With advanced manufacturing technologies, the assembly boundaries between parts do not necessarily need to be planar or orthogonal. Thus, there is an increased need for a design tool to help designers explore the full design space of constraint configurations so as to enable more informed design decisions that can ultimately yield superior assembly designs.

The majority of previous work on optimal constraint design is in the area of workpiece fixturing. These studies mainly aim to provide more robust clamping strategies [2–4]. De Meter [2] investigated the optimization of locating feature positions and clamp intensities for maximizing mechanical leverage and minimizing deformation. The approach seeks to minimize the maximum normal load within the search space of the independent variables using a feasible direction technique that satisfies the Fritz-John necessary local optimality condition. Cai et al. [3] used a variational method to accomplish the same goal via closed-form mathematical solutions. In contrast to finite element approaches, this method provides for easier physical interpretation of and insight into the fixture configuration behavior. The constraint equations are derived from requirements to maintain contact with all locators and minimize position and orientation errors. Simple 2D and 3D examples show initial configurations and optimized configurations with reduced error. Chou et al. [4] extended the robotic grasping work of Lakshminarayana [5], Salisbury and Roth [6], and Kerr and Roth [7] to fixture design in specifying equations for deterministic location, clamping stability, and total restraint. For $n \geq 7$, the clamping force solutions are homogeneous and similar to what Salisbury and Roth [6] called internal forces. A similar effort by Hirai and Asada [8] also represented these design requirements as simultaneous inequalities in terms of inner products of two vectors and created a solution via the theory of polyhedral convex cones. The work by Asada is also extended by Xiong et al. [9] to include force determinacy and relative form closure which is then added with an analysis of inner force distribution and load carrying capacity of the fixture grasps.

Contributed by the Design for Manufacturing Committee of ASME for publication in the Journal of Mechanical Design. Manuscript received October 21, 2012; final manuscript received April 11, 2013; published online May 24, 2013. Assoc. Editor: Rikard Söderberg.

While the optimization conditions common in fixturing, such as maintaining contact with locators, are also applicable in assembly constraint design, the load wrenches, which are typically known or at least adequately modeled in fixturing, can be arbitrary in assembly design. No clamping forces are applied in assembly, so the homogenous solution approach to solve for internal forces at the constraint features cannot be applied. Additionally, in the context of the problem presented in this paper, positional accuracy is of relatively less interest compared to assembly resistance to loading wrenches. Marin and Ferreira [10–12] addressed the synthesis of optimal clamping locations on 3D parts with planar and cylindrical faces. They solve the optimization problem given a part with predefined deterministic locators, a set of polygonal convex regions acting as the admissible clamping areas, and a known set of external disturbing wrenches. Since the optimal solution may not be unique, they identify lines of constant clamping force, along with clamps that can be moved while maintaining a constant clamping force. In mechanical assembly, a line of constant clamping force is analogous to a line along which constraints can slide without any change in forces at the constraints. Ding et al. [13] approach the same optimization problem with quadratic programming with workpiece positioning accuracy as the performance index and form-closure requirement as the linear constraints.

Schimmels [14] developed a model to evaluate the space of allowable motion in workpiece fixturing. Similar to work by Asada and By [15], he defined a linearly force assemblable fixture using the principle of virtual work. A fixture is deterministic if the constraints of a partial fixture provide N independent wrenches when the workpiece is located in its properly mated position. Three linearly independent contact wrenches are required for a planar fixture, and six are required for a spatial fixture [16]. Schimmels also examined detachable fixtures for which at least one unconstrained trajectory, or detaching motion, exists between the desired workpiece location and an outside position [14].

Lee et al. [17] proposed a methodology to synthesize flexible fixture workspaces for a set of different stampings as opposed to only a single loading. The methodology involves representing the candidate locator region from the fixture robot workspace and optimizing the objective function, which is a function of circle size and overlap, via a genetic-algorithm-based probabilistic search. Lee and Haynes [18] also explicitly included part stiffness in optimizing fixture elements using finite element methods. The workpiece is modeled as a linearly elastic deformable body with coulomb friction, and the optimization minimizes the total work done on the workpiece. A similar effort by Menassa and DeVries [19], also using finite element methods, proposes optimization techniques for minimizing workpiece deflection at selected points. Gui et al. [20] applied a similar elastic workpiece model with the end goals of improving location accuracy and minimizing error. These various approaches are useful for a single optimization, but lack a means to explore the design space of mechanical assembly constraints.

Design of statically determinate assemblies [21,22] and exact constraint design [23,24] are well known in the mounting of precision instruments and tools. Slocum [21] identified two important principles for precision structural designs: kinematic design and elastic averaging. The principle of kinematic design states that point contact should be established at the minimum number of points required to constrain a body in the desired position and orientation. Preventing overconstraint enables exact mathematical modeling, so the mounting or attaching of parts via kinematic design is repeatable and precise. In this way, kinematic design is analogous to form closure because its main concern is deterministic location of the part. High contact stresses that limit load capacity, however, are common, so the principle is generally not employed when large service wrenches are anticipated. Redundant contact points are needed to support larger loads, in which case a set of compliant couplings is used. The principal of elastic averaging employs a large number of contact points spread over a broad region to support a large load uniformly. The weakness of this approach is that the location of the part becomes indeterminate. In this way, elastic averaging design is analogous to force closure because by redundantly supporting the part, its location is not deterministic. Downey et al. [25] recommends the use of smart assembly features to absorb manufacturing variation while still maintaining critical dimensions of the final assembly. By using these smart features, classified based on the DOF allowed to absorb variation, nesting forces usually required in exactly constrained can be provided without adding redundancy to the constraint configuration. To predict the influence of various locating, clamping, and joining features on final assembly variation, Soderberg et al. [26] presents an analysis tool integrated with various Computer Aided Design (CAD) softwares. This tool allows the designer to identify variations that will critically influence problems later in final assembly production.

Many mechanical assemblies in consumer products do not require the accuracies offered by kinematic design and are more prone to arbitrary loading in fulfilling their functions. Typical assemblies inevitably require redundant constraints, but they are not necessarily designed properly according to elastic averaging principles. As a result, overconstrained designs often result in high preload or loose fit due to dimensional variation in manufacturing. Because reaction forces are statically indeterminate, there is a need for design tools that extend the use of elastic averaging principles to achieve insensitivity to manufacturing variations.

Whitney and his colleagues [27,28] are among the few researchers who have addressed assembly design by laying out principles for designing constraint configurations. They present a theory of designing assemblies to deliver key characteristics (KC), which are geometrical relationships critical to achieving functional customer requirements. A datum flow chain (DFC) is created to trace geometrical links between assembly parts [29], identifying joints between parts that pass important constraints (called "mates") and joints that do not pass constraints (called 'contacts'). In assembly design, using KC and DFC enables engineers to identify important connections in a multipart assembly. Adams et al. [30,31] provided a design tool to implement Whitney et al.'s concepts [28] using screw theory to determine the level of constraint, either underconstrained or overconstrained, and to identify any unconstrained motions. This analysis, however, offers no quantitative metric of the constraint effectiveness of a mechanical assembly. Since most mechanical part assembly is already overconstrained, the design tool cannot be used to analyze the effectiveness of a constraint configuration.

Rusli et al. [32] developed an analysis technique based on screw theory that provides a quantitative rating for mechanical assemblies. This paper demonstrates how that analysis work can be used as a design tool for constraint optimization. A summary of the analysis approach and an additional assembly performance metric are provided in Sec. 2. This metric serves as the objective function for the optimization in the design tool. The main contribution of this paper is the optimization tool that leverages the analysis algorithm to explore the design space of an assembly feature's location and orientation provided by the designer (Sec. 3). This ability to optimize an individual feature or set of features is then expanded to a multidimensional design space by taking factorial combinations of assembly features to optimize the assembly's overall constraint configuration (Sec. 4). This is important because of interaction effects among individual constraint features. Because the design decisions may involve tradeoffs between assembly resistance to motion and redundancy that vary with context, the tool also provides the designer with the ability to increase/decrease the number of assembly features (Sec. 5).

In this paper, the word "optimum" is used to refer to an optimal point within the design search space provided by the designer. Because the search algorithm is discrete rather than continuous, there may be superior points in between the discrete locations, but this can be resolved by increasing the search resolution.

2 Methodology and Assembly Rating Metrics

The quantitative rating of mechanical assemblies that provides the foundation of the design optimization in this paper is based on

Table 1 Sample rating matrix

	C_1	C_2	C_3	C_4	C_5	C_6	C_7	C_8	Shared resistance
Motion 1	0	0	0	0	0	0.802	1.031	1.018	2.851
Motion 2	0.369	0	0	1.495	0	0	0.716	0	2.580
Motion 3	0	0	0.775	0	0.796	0	0	0	1.571
Motion 4	0	0.946	0	0.057	0	0.798	0	0	1.801
Motion 5	0	1.120	0	0	0	0	1.296	1.200	3.616
Motion 6	1.159	0	0.903	0	0	0	0	0.590	2.652
Motion…	—	—	—	—	—	—	—	—	—

modeling the assembly constraint features as one-system, two-system, and three-system wrenches in screw theory [32]. By taking multiple combinations of constraint features that compose up to a five-system (called the pivot constraints), a unique reciprocal screw motion that is unconstrained by the five-system can be generated. The remaining constraints that do not belong to the pivot constraints act as reaction constraints that provide resistance to the evaluated motion. These individual resistance values, which describe the effectiveness of individual constraints to a certain motion, can be rated individually and arranged in a matrix. The rows correspond to the m evaluated motions, and the columns correspond to the n evaluated constraints. The reaction force magnitude at the constraints to resist an input wrench with unit magnitude is calculated to fill the $m \times n$ matrix. Because a small reaction force signifies good resistance quality while a large reaction force signifies low resistance quality, the reaction force magnitude is not immediately intuitive for the user. In order to make the interpretation of these values straightforward for further processing, a reciprocal $(1/x)$ of each matrix cell value is taken. After the reciprocal, A smaller value signifies a weakly constrained motion, while a larger value indicates a strongly constrained motion. Table 1 shows a sample rating matrix with eight constraints (C_1 through C_8). The nonzero resistance values are the constraints that actively resist the respective motion.

To consider the shared resistance (SR) quality of a constraint configuration, the individual resistance values of all the constraints for the specific motion are summed. This value, the last column in Table 1, is called SR. To use this sum for assembly evaluation, several rating metrics are derived. The first rating metric, the weakest shared resistance (WSR) rating, measures an assembly's performance based on its capability to resist the most weakly constrained motion. It is the minimum value among the shared resistance values of all the evaluated motions. This is appropriate since an assembly may be considered only as good as its weakest motion resistance. In the sample rating matrix in Table 1, the WSR value is 1.571, coming from motion 3. The second rating metric, the mean shared resistance (MSR) rating, is the average of the shared resistance values for all motions, which characterizes resistance quality to arbitrary motion. Two constraint configurations with identical WSR ratings could differ substantially in overall effectiveness as measured by MSR. For the six motions listed in Table 1, the MSR value is 2.512.

In order to quantify the trade-off between assembly resistance capacity and redundancy, two other rating metrics, mean resistance redundancy (MRR) and trade-off ratio (TOR), can be defined. The redundancy ratio for each motion is the ratio between the shared resistance value (sum of a row) and the peak resistance value (maximum of a row). It quantifies the degree of resistance to a specific motion available relative to exact constraint by the single most effective constraint. In Table 1, the constraints that actively resist motion 5 are C_2 (1.120), C_7 (1.296), and C_8 (1.200), so the redundancy ratio is 2.790. MRR, then, is the average of the redundancy ratios of all motions in the rating matrix, with a minimum MRR value of unity indicating exact constraint and larger values indicating greater redundancy. The TOR is the ratio of MSR to MRR. By observing the change in TOR as the design space is searched, the designer can select designs that yield the greatest resistance quality with minimal redundancy. For the six motions listed in Table 1, the MRR value is 2.241, so the TOR value is 1.121.

3 Optimization of Constraint Location and Orientation

Theoretically, there are infinitely many ways to remove DOF between two bodies using constraints. Although there are geometrical limitations on constraint location, orientation, and size imposed by manufacturing considerations, much of the design search space is often unexplored because nonrectilinear motion constraints are not intuitive to designers. One of the central functions of the design tool is to inform the designer of possible improvements in constraint locations and orientations within the search space. Because constraints are also provided at the part boundaries, the improvements could yield more efficient part boundaries in an assembly that are not necessarily typical planar splits between part halves. Specific constraint features can be idealized and modeled as points, pins, lines, and planes, and the different design search spaces for each are shown in Table 2. These search spaces are as follows:

- The "discrete locations" search space is a set of discrete candidate point locations for the constraint variable. For a pin, line, and plane constraint, the center point of the constraint defines the location.
- The "along a line segment" search space is defined by its center point L_o, its direction vector $\vec{L}_d$, and the move limits specified in either direction δ. For pin, line, and plane constraints, the center point is moved along this line segment.
- The "along an arc" search space is defined by its center point L_o, its rotation axis $\vec{L}_R$, and the angular move limit in either direction θ.
- The "within a plane" search space is defined by its center point P_o, its two principal direction vectors $\vec{P}_x$ and $\vec{P}_y$, and the move limits in either direction for both axes δ_x and δ_y.
- The orientation search space is defined as the rotation of the normal vector of the constraint about one or two axes within a certain angular magnitude called the angular move limit.
- The line length search space is defined as the length of the line constraint.
- The plane area search space is defined by the length and width of the plane constraint.

Table 2 Design space mapping for each constraint type

	Location Search Space				Orientation search space	Size search space	
Constraint type	Discrete locations	Along a line segment	Along an arc	Within a plane	Normal direction	Length	Area
Point	√	√	√	√	√		
Pin	√	√	√	√	√		
Line	√	√		√		√	
Plane	√	√		√	√		√
Search space dimension	1D	1D	1D	2D	1D or 2D	1D	1D

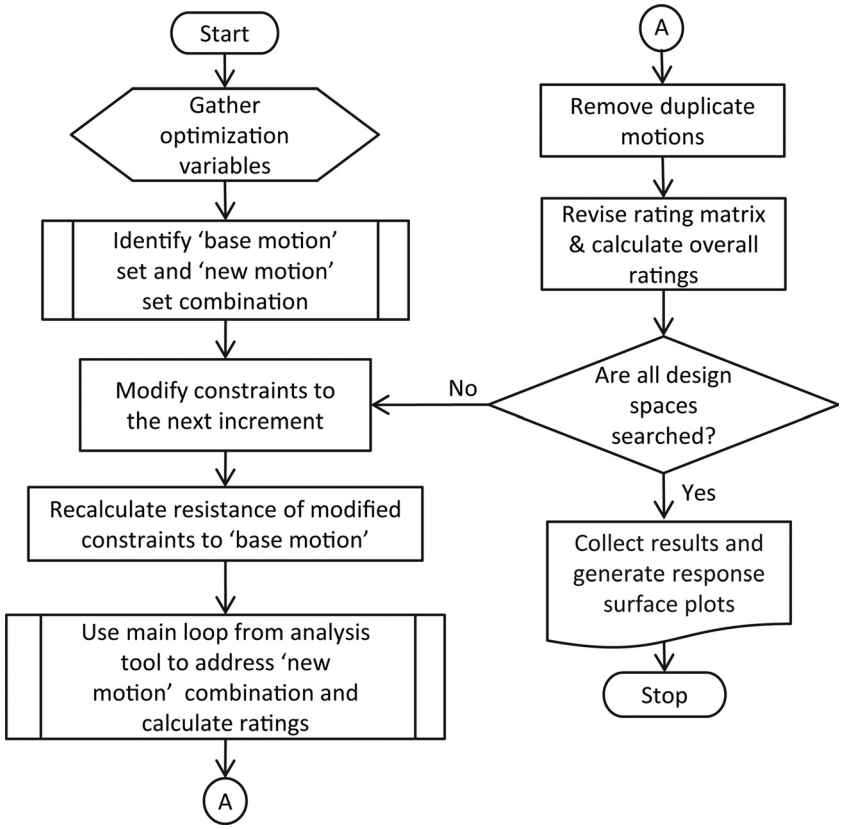

Fig. 1 Simplified flowchart for constraint modification algorithm

The design tool presented can be used to search all of the spaces listed in Table 2, although they are not all presented in this paper.

3.1 Constraint Modification Algorithm. While a specific algorithm was developed for each search space combination, the general constraint modification algorithm is shown in Fig. 1. The goal is to calculate the change in assembly rating as the locations, orientations, and sizes of constraints are modified.

Since one physical assembly feature may be represented by multiple mathematical constraints, constraint modification needs to be done in groups. For example, a small alignment tab or lip feature might provide translational constraint in two directions. As this feature is modified, the constraints that are a subset of this physical feature are grouped and modified (moved, re-oriented, or resized) simultaneously. After the search space for a constraint group is defined, it is discretized into increments along the search dimension(s). The variable x is the increment along each search dimension and is normalized to have a range of $-1 \leq x \leq 1$, with -1 and 1 corresponding to the minimum and maximum move limits. In the case studies, the number of increments is typically set to 10 or less to maintain a realistic computation time while still yielding enough data points to plot the optimization results.

Recall that the evaluated motion set is generated from a set of wrench five-systems taken from the pivot constraints, selected in turn using a combination scheme. This motion set is resisted by the remaining constraints called the reaction constraints. Because of this, any modification to the constraint configuration also modifies the evaluated motion set. In this sense, the constraint modification algorithm is recursive. When constraints are modified, there are two cases of recalculations involved in the process:

(1) When the modified constraints are part of the pivot constraints, a new motion set is generated by solving Eq. (1) for the new motion reciprocal to the revised pivot wrench set $\vec{C}_{P1,P5}$, solving for the new reciprocal motion

$$\left[\vec{C}_{P1,P5}\right]\begin{bmatrix}\vec{\mu}\\ \vec{\omega}\end{bmatrix} = \left[\vec{0}\right] \tag{1}$$

(2) When the modified constraints are part of the reaction constraints, the motion set does not change, but the resistance quality of each motion is recalculated. This process involves revising the reaction wrench $\vec{C}_{\mathrm{R}}$ in

$$\vec{C}_{\mathrm{R}} = \begin{bmatrix}\vec{R} \times \hat{N}\\ \hat{N}\end{bmatrix} \tag{2}$$

and resolving the equilibrium

$$\left[\vec{C}_{P1,P5}, \vec{C}_{\mathrm{R}}\right][\lambda_{\mathrm{i}}] = -\vec{L}$$

where $\vec{L}$ is the input wrench and λ_{i} is the reaction force intensity.

These recalculations are done for each iteration of the algorithm, which serves as an increment of constraint modification in the search space. A revised rating matrix is created by merging the results from the recalculation procedures, and the overall assembly rating is calculated. The change in assembly rating is reported as a response curve for a 1D search and a response surface plot for a 2D search to provide design space information to aid design decisions. For visualization purposes, the search space dimensions in the following case studies are limited to two at a time. In each response curve, X1 and X2 refer to the normalized independent variables, and the vertical axis refers to the labeled rating (WSR, MSR, etc.).

3.2 Constraint Modification Case Study. The case study is focused on an assembly for which the constraint design space is

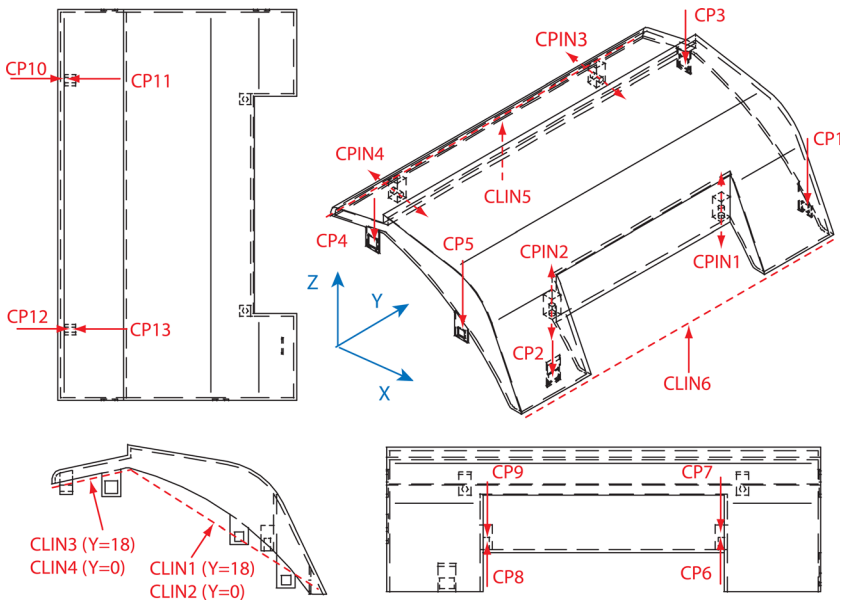

Fig. 2 Printer housing geometry and assembly constraints

not necessarily intuitive for a designer due to complex, freeform part geometry and nonrectilinear constraint orientations. The Epson Stylus C82 printer housing assembly in Fig. 2 is constrained by four threaded fasteners, five cantilever snap-fits, and a tongue and groove feature along the perimeter edges of the part. The threaded fasteners are modeled as pin constraints with two unilateral point constraints along the fastener's axis in opposite directions (CPIN1 through CPIN4). The pin constraint is due to the fastener's pin geometry, and the two-way point constraints (CP6 and CP7) are due to the locking of the threads. The total DOF removed by a single threaded fastener feature is 3 (all translation DOFs). The snap-fits mainly remove a one-way DOF along the beam length direction and are modeled as unilateral point constraints (CP1 through CP5). The tongue and groove lines are divided into segments of line constraints in its vertical assembly direction (CLIN1 through CLIN6). The ribs in the tongue and groove feature are neglected altogether in the model because their low stiffness in the XY plane compared to the unilateral constraint in the z-direction mean they do not necessarily serve as constraints that remove DOF.

For all instances of this case study, the objective is to maximize the WSR rating so as to improve performance with regard to the assembly's most weakly constrained loading direction. When there is no change in the WSR rating, maximizing the MSR rating becomes the secondary objective to improve performance with regard to arbitrary loading conditions. In searching for optimal designs, the manufacturability and cost of the improved design are not explicitly considered here, but could be readily included as constraints on the search space. Also, for visualization purposes, the optimization for each design space is limited to a two-dimensional search. These localized design spaces are individually searched in sequence, and then, the design spaces in which possible improvements are identified are merged and searched simultaneously to yield an improved design recommendation for the housing in Sec. 4.

The design space for each optimization study is summarized in Table 3 and discussed in detail in Sections 3.2.1 through 3.2.3.

3.2.1 Optimization of Threaded Fastener Location and Orientation. The design space for the threaded fastener locations is searched by allowing the location of all four fasteners to move along two lines. The threaded fasteners at the locations of CPIN1 and CPIN3, as well as those at CPIN2 and CPIN4, are linked to move together so as to reduce the dimension of the optimization search. Thus, Table 3 specifies two groups of variables. The first group (X1) involves the two fasteners near the bottom of the housing, so the constraints in this group are CPIN1, CPIN3, CP6, CP7, CP10, and CP11. The second group (X2) consists of CPIN2, CPIN4, CP10, CP11, CP12, and CP13. The move limits for these variables are selected based on the physical limitation of the part size.

The WSR plot in Fig. 3 shows that the rating cannot be increased from the baseline model. The WSR rating is relatively constant for cases in which the two groups of fasteners are located symmetrically, whereas it decreases for cases in which the threaded fasteners are not equidistant from the part symmetry line. Although the spreading of the fastener should increase the individual rating of the modified fastener, the WSR motion only evaluates motion resistance for one particular motion, namely, the most weakly constrained one. If the WSR motion changes after the fastener is moved, it is possible that the rating stays constant. The MSR plot also shows no improvement possible in this design space. The discontinuity in the MSR plot is due to the fact that when two fastener locations coincide or nearly coincide with one another, there are motion sets that are eliminated or added due to linear dependency that occurs in the combination.

The orientation design space for the threaded fastener listed in Table 3 is explored by allowing the orientation of all four fasteners to rotate about the x- and y-axes. The response surface plot shown in Fig. 4 indicates that the WSR rating can be increased by up to 24.6%. The rating reaches a maximum value for X1 rotations of ± 72 deg and X2 rotations from 36 to 53 deg or -36 to -53 deg, all about the y-axis. A more detailed examination shows that the rating improvement results from a change in the most weakly constrained motion as the fasteners are re-oriented. The cost of this design would likely be greater than the baseline design because the change would require sliding cores for the CPIN1 and CPIN2 fasteners in the injection mold that are tilted at an angle other than 90 deg. Note that the baseline design already has sliding cores for fasteners CPIN3 and CPIN4. If this cost increase is not acceptable, an improved design in which CPIN3 and CPIN4 are rotated while CPIN1 and CPIN2 remain the same still offers an improvement of approximately 12%. Because this kind of assembly improvement is more difficult for a designer to visualize, it is where the design tool can prove most useful.

3.2.2 Optimization of Snap-Fit Location and Orientation. The design space for the snap-fit location specified in Table 3 is searched by allowing the locations of four snap-fits

Table 3 Summary of constraint modification search space parameters

Threaded fastener location	Parameter	Variables	Line search center	Line direction	Move limits
	X1	CPIN1, CPIN3, CP6, CP7, CP10, CP11	[8.625 9 1.744]	[0 1 0]	$-4.875 \leq x_1 \leq 4.875$
	X2	CPIN2, CPIN4, CP8, CP9, CP12, CP13	[8.625 9 1.744]	[0 1 0]	$-4.875 \leq x_2 \leq 4.875$
Threaded fastener orientation	**Parameter**	**Variables**		**Rotation axis**	**Angular limits**
	X1	CPIN1, CPIN2, CP6, CP7, CP8, CP9		[0 1 0]	$-90\,\text{deg} \leq \theta_1 \leq 90\,\text{deg}$
	X2	CPIN3, CPIN4, CP10, CP11, CP12, CP13		[0 1 0]	$-90\,\text{deg} \leq \theta_2 \leq 90\,\text{deg}$
Snap-fit location	**Parameter**	**Variables**	**Line search center point**	**Search direction**	**Move limits**
	X1	CP1, CP5	[7.125 18 3.200]	[−3.093 0 3.441]	$-4.5 \leq x_1 \leq 4.5$
	X2	CP3, CP4	[1.551 18 4.754]	[2.000 0 0.431]	$-1.5 \leq x_2 \leq 1.5$
Snap-fit orientation	**Parameter**	**Variables**		**Rotation axis**	**Rotation angle limits**
	X1	CP1, CP5		[0 1 0]	$-60\,\text{deg} \leq \theta_1 \leq 60\,\text{deg}$
	X2	CP3, CP4		[0 1 0]	$-60\,\text{deg} \leq \theta_1 \leq 60\,\text{deg}$
Parting line orientation	**Parameter**	**Variables**		**Rotation axis**	**Rotation angle limits**
	X1	CLIN1, CLIN2		[0 1 0]	$-60\,\text{deg} \leq \theta_1 \leq 60\,\text{deg}$
		Variables	**Line search center**	**Search direction**	**Move limits**
	X2	CLIN5, CLIN3, CLIN4, CPIN3, CPIN4, CP3, CP4, CP10, CP11, CP12, CP13	[0 9 3]	[0 0 1]	$-1 \leq x_1 \leq 1$

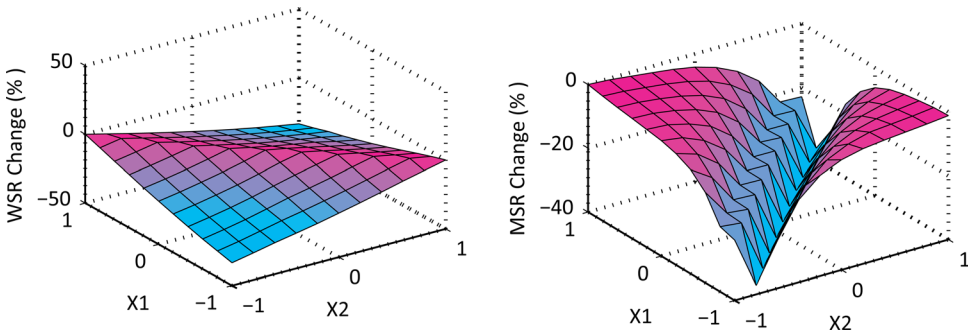

Fig. 3 Response surface plot for fastener location optimization

(CP1 andCP5 as variable group X1, CP3 and CP4 as group X2) to move along lines defined by the edges. The WSR rating does not change for any value of the optimization variables because the constraints being optimized are not active in resisting the most weakly constrained motion. Therefore, consideration of the MSR rating drives the optimization instead, and the response plot in Fig. 5 shows that it increases (4.5%) as the constraints CP1 and CP3 are moved higher along the line. The maximum MSR rating occurs where CP1 is located between the coordinates [5.320 18 5.208] and [5.922 18 4.539] along the line

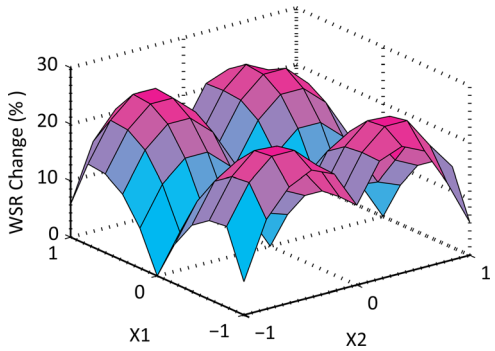

Fig. 4 Response surface plot for fastener orientation optimization

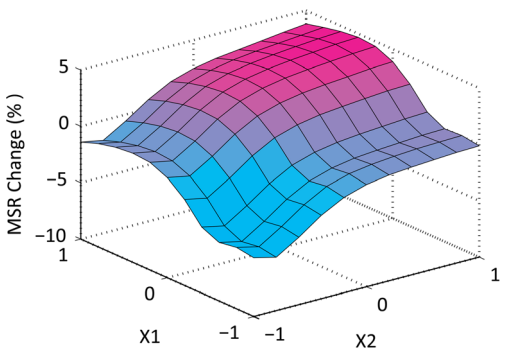

Fig. 5 Response surface plot for snap-fit location optimization

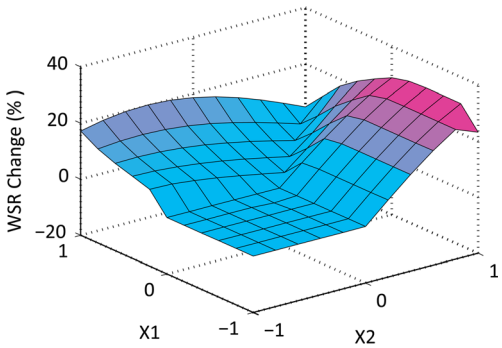

Fig. 6 Response surface plot for snap-fit orientation optimization

search. It is difficult to isolate one particular reason that moving CP1 down and CP3 up not yielding an optimal result. If the geometry is constrained by these four snap-fits alone, then this would be intuitive and obvious. However, there are many other constraints that resist motion in the Z-axis translation, namely, CPIN3, CPIN4, CP6, CP7, CP8, and CP9, to name a few. All of these constraints are working together to contribute to the MSR rating. While it might not be apparent to the designer that the best location for the snap-fits is as advised in the optimization results, this is where the design tool fulfills its purpose, namely to provide design knowledge where simultaneous effects of many constraints are in place.

The design space for the snap-fit orientation specified in Table 3 is searched by allowing the orientations of four snap-fits (CP1, CP3, CP4, and CP5) to rotate around the *y*-axis. Again to reduce the dimension of the search, CP1 and CP5 are linked and rotated together, as are CP3 and CP5. The response surface plot in Fig. 6 has two local maxima, so a WSR rating increase of 20–30% is achievable by re-orienting the snap-fits. In order to improve the rating, the orientations of the paired snap-fits CP1 and CP5 must be rotated 60 deg around the rotation axis and the orientations of CP3 and CP4 rotated 30 deg in the opposite direction about the same axis. From an assembly point of view, however, this is not possible unless the part is divided into two pieces and their assembly directions changed.

3.2.3 Optimization of Parting Line Orientation. The design space for the parting line specified in Table 3 is searched by allowing the orientations of line constraints CLIN1 and CLIN2 to be rotated about the *y*-axis. Rotating the orientation of the parting line, however, requires that CLIN3, CLIN4, CLIN5, and the two fasteners follow the parting line change by moving along the *z*-axis. Ideally, the two search spaces would be linked geometrically, but this is not possible in the current design tool software, so they are treated as two independent design variables. The second variable group does not involve rotating the parting line, but rather searching the location of the parting line in the *z*-direction.

The response surface plot in Fig. 7 shows that the WSR rating is only affected by the orientation of CLIN1 and CLIN2 and not by changes in the X2 variables. As CLIN1 and CLIN2 are rotated closer to the horizontal plane, the WSR rating decreases significantly, whereas rotating CLIN1 and CLIN2 in the opposite direction yields no gain in the rating.

While moving the position of the second group of variables in the *z*-direction does not affect the WSR rating, the effect on the MSR rating is significant. The MSR plot in Fig. 7 shows that not only does rotating the parting line toward the XY plane decrease the rating, but so does lowering the position of the second group of variables in the *z*-direction. If the printer housing were designed with a typical planar parting line (X1 = −1), the rating would be much lower, by as much as 23.3% in the WSR rating.

Based on these optimization studies, it is shown that significant design improvements are possible by relocation and/or reorientation of the constraints within their search spaces. The advantages of a nonrectilinear parting line are also demonstrated.

4 Multidimensional Search for Synthesis of Improved Overall Design

While each of the potential design improvements outlined in Sec. 3.2.2 could be implemented individually, the interaction effects when design changes involving multiple variables occur simultaneously may be positive or negative. To understand these interactions in larger and more complex constraint configuration changes, the individual design spaces are combined as full factorial experiments similar to a design of experiment (DOE) method with a total search dimension equal to the sum of all combined search space dimensions. The limitation of such higher dimensional optimization is mainly in computational power and the efficiency of the design tool software. Because the objective function cannot be expressed as an analytical function, it is not possible to employ typical optimization methods. Currently, the tool allows up to a five-dimensional search with about six levels in each dimension. The variables identified for improving the printer housing assembly are

- Orientations of two threaded fasteners ({CPIN1, CPIN3, CP6, CP7, CP10, CP11},{CPIN2, CPIN4, CP8, CP9, CP12, CP13})(2D search)
- Orientations of four snap-fits (CP1, CP3, CP4, and CP5) (2D search)
- Locations of two snap-fits (CP1 and CP3) (1D search)

The merged search space and optimization results with respect to WSR are shown in Table 4. Specifically, the X3 and X4 constraint orientations are rotated in the opposite direction compared to the previous results in Fig. 6 and the X5 constraint positions of CP1 and CP5 are shifted in the opposite direction compared to the previous results.

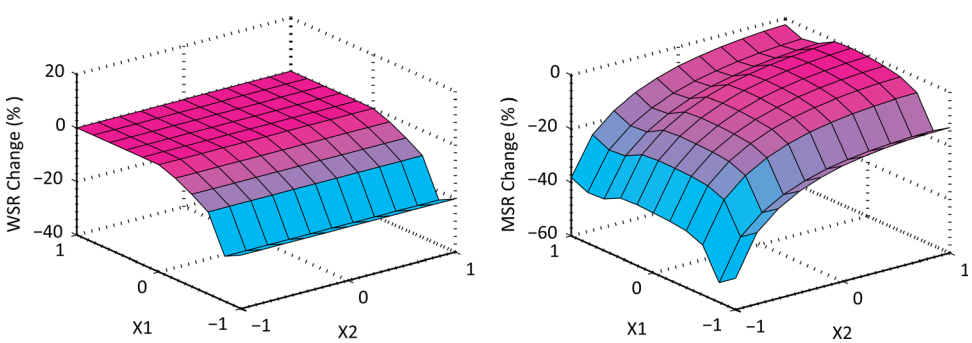

Fig. 7 Response surface plot for parting line optimization

Table 4 Multivariate design search space and optimal constraint configuration

	Normalized units	Optimization variables	Search type	Design change
X1	−1.0 or 1.0	CPIN1, CPIN2, CP6, CP7, CP8, CP9	Orientation	Rotate CPIN1, CPIN2, CP6, CP7, CP8, and CP9 90 or −90 deg about the *y*-axis
X2	−0.6	CPIN3, CPIN4, CP10, CP11, CP12, CP13	Orientation	Rotate CPIN3, CPIN4, CP10, CP11, CP12, and CP13 −54 deg about the *y*-axis
X3	0.6	CP1, CP5	Orientation	Rotate CP1 and CP5 54 deg about the *y*-axis
X4	−0.6	CP3, CP4	Orientation	Rotate CP3 and CP4 −54 deg about the *y*-axis
X5	−0.6	CP1, CP5	Location	Move CP1 to [7.526 18 2.754] and CP5 to [7.526 0 2.754]

Table 5 Summary of design improvement ratings

	WSR		MSR	
	Rating	% Diff.	Rating	% Diff.
Baseline design	2.437	0.0	17.628	0.0
Fastener reorientation	3.036	24.6	17.203	−2.4
Snap-fit reorientation	3.180	30.5	18.827	6.8
Snap-fit relocation	2.437	0.0	18.421	4.5
Combined design space modification	3.507	43.9	18.323	3.9

The result shows the presence of interaction effects in that the optimal constraint configuration does not match any of the individually optimized results. Table 5 summarizes the design improvements across the possible design revisions. It is found that the optimum (combined design space modification) has the best WSR rating. Furthermore, the rating gains obtained by individual design changes do not always accumulate when all of them are implemented. Because of such interactions, the design space exploration should be treated as a DOE problem. In this particular case study, the interaction between orientation design spaces is more likely compared to interaction between location and orientation design spaces or between location design spaces. Because the best design is the one that yields the most assembly rating increase with minimal cost of design implementation, the study can be further implemented in a rating metric that measures the trade-off ratio between assembly resistance quality and cost of design implementation (i.e., dollar per additional features).

5 Trade-Off Study Between Assembly Resistance Quality and Redundancy

Beyond optimizing individual constraint locations and orientations, identifying an optimal number of constraints in an assembly is critical to reduce part complexity, the number of required fasteners, and ultimately, product cost. Using more constraints generally leads to a stronger and more reliable assembly since a broader distribution of loads reduces reaction forces. On the other hand, more constraints also increase redundancy. While redundant designs, when done properly, can provide greater load carrying capability, they have important drawbacks such as increased part-to-part variation as manufacturing tolerance can lead to either locked-in stresses or loss of contact between the part and the constraints. The design tool can provide data for the designer to manage the trade-off balancing any increase in internal stresses and preload with overall assembly strength and resistance quality. An optimal design is located at the point where an assembly's resistance capacity is maximized with minimal increase in redundancy. The MRR and TOR are useful metrics in the following examples that first examine constraint reduction and then constraint addition.

5.1 Constraint Reduction Trade-Off study. The constraint reduction algorithm iteratively removes both individual constraints and combinations of constraints, calculating the resulting assembly rating in each case. The results are displayed as a bar graph of TOR values for each removal scheme denoted by a constraint removal index. When only one constraint is removed, the index is identical to the constraint number, and when constraints are removed simultaneously, the index is mapped to the particular combination. The scheme that yields the maximum percentage increase in the TOR value is considered optimal.

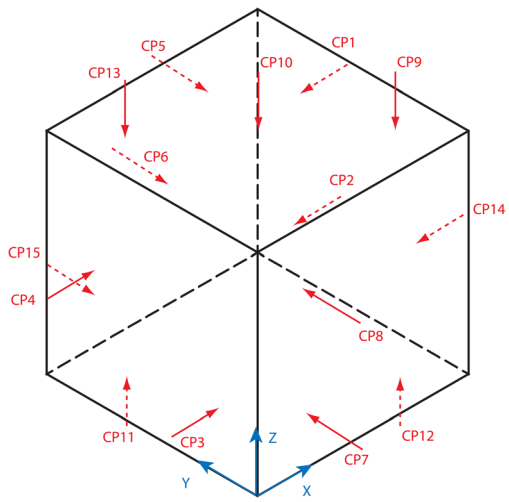

Fig. 8 Cube constraint configuration

For this case study, the geometry is a 1 in. × 1 in. × 1 in. cube with 15 point constraints at various locations across all six faces (Fig. 8).

Figure 9 shows a plot of the TOR rating change as each constraint is removed one at a time. When the TOR value is not plotted, the assembly loses total restraint or has become underconstrained.

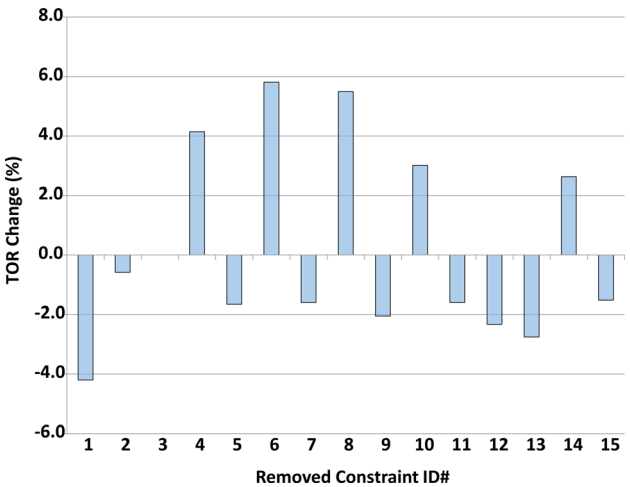

Fig. 9 Rating change due to constraint removal (one at a time)

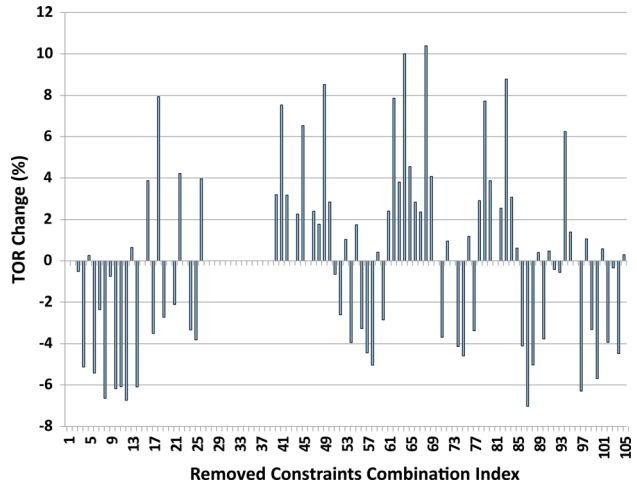

Fig. 10 Rating change due to constraint removal (two at a time)

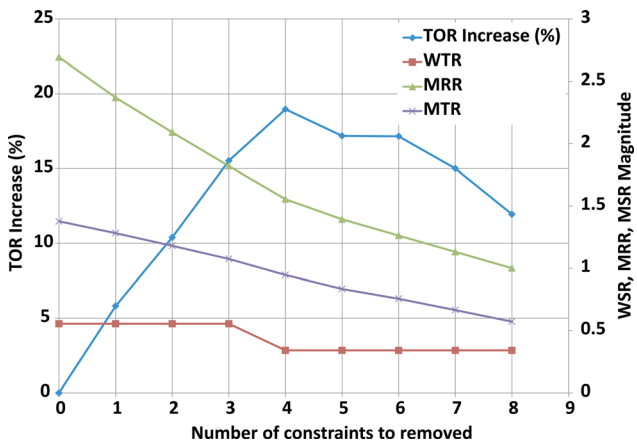

Fig. 11 Overall rating change as constraints are removed

Constraints that have a negative impact on TOR when removed are ones that add more strength than redundancy, so it is desirable to retain them. Constraints that have a positive impact on TOR when removed (CP6, CP8, CP10, and CP14) add more redundancy than strength, so they are candidates for removal. CP3 is the most critical constraint since it cannot be removed without the assembly losing total restraint, as indicated by the omission of a plotted TOR change for constraint removal index 3. In contrast, removal of CP6 offers the greatest percent increase in TOR.

These results are only valid when one constraint is removed. When two constraints are to be removed, the constraint removal algorithm needs to be done for all possible combinations. Figure 10 plots TOR changes for all 105 combinations of two simultaneously removed constraints.

Note that for many indices, the assembly loses total restraint. This is true for every constraint removal combination involving CP3 and for a few other combinations. The simultaneous removal of constraints CP6 and CP14, denoted as index #68, yields the maximum percent increase in TOR, due at least in part to CP6 and CP14 being linearly dependent on the rest of the constraint configuration, which increases redundancy. The case study can of course be extended to remove more simultaneous constraints.

Figure 11 plots the values of the various metrics for the constraint removal schemes that produce the largest percent TOR increase for removal of up to eight constraints (the maximum possible).

Note that there are two vertical axes on the plot. The left side axis is for the TOR increase (%), while the right side is for the WSR, MRR, and MSR ratings. The first set of results is the baseline design (no constraint removed). It can be observed that as more constraints are removed at a time, the assembly ratings WSR, MRR, and MSR monotonically decrease. MRR reduces to 1.0 when only seven point constraints remain, which is expected for an exactly constrained assembly. The maximum possible gain in TOR increases through removal of up to four constraints at a time (19% increase) and decreases afterward. This means that removing five constraints from the assembly does not yield a better TOR compared to removing four constraints. In other words, a pattern of diminishing return occurs in the context of optimizing the assembly by reducing redundancy. In using the constraint reduction scheme, one should be careful to note that the overall assembly ratings (WSR and MSR) do not decrease beyond acceptable limits.

5.2 Constraint Addition Trade-off Study. In the constraint addition algorithm, the user specifies the constraint types to be added and their locations and orientations. The algorithm adds these constraints one at a time and recalculates the assembly rating change. The geometry used for this case study is the end cap for a medicine spray housing shown in Fig. 12. Locking is provided by two cantilever snap-fits located symmetrically at the lips of the end cap assembly, and the part is constrained by a pin and a plane constraint, both provided by the lip mating interface. The

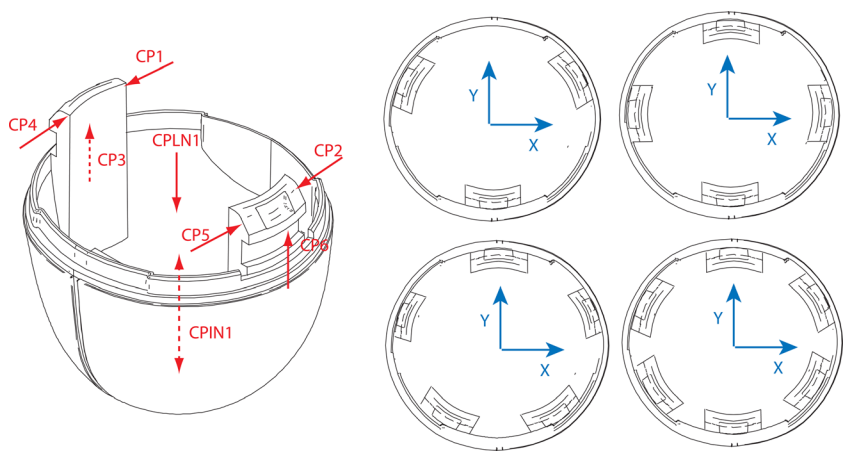

Fig. 12 Endcap geometry and constraint feature additions

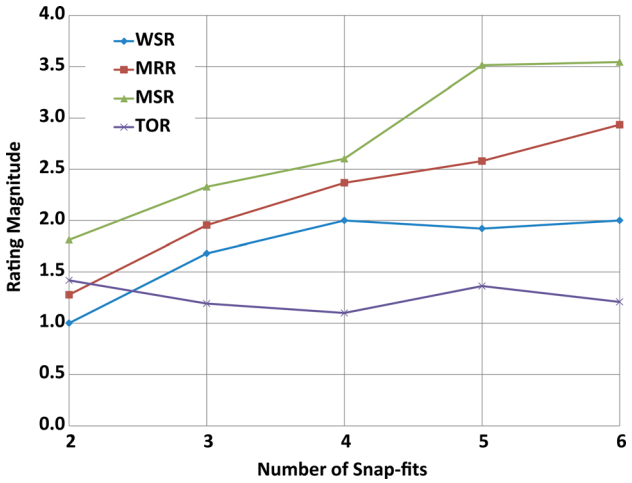

Fig. 13 Rating change as the number of snap-fits is increased

constraint features to be considered for addition are more snap-fits around the lip of the end cap.

Figure 13 shows that adding snap-fit features yield gains in WSR and MSR at the cost of additional redundancy as measured by the MRR value. Due to these simultaneous increases, the TOR remains approximately constant. Adding more than four snap-fit features does not yield any significant gain in WSR rating, and beyond five snap-fits, there is no significant gain in either WSR or MSR. This study is useful in determining the point at which adding more constraints yield diminishing returns. The design recommendation is to increase the number of snap-fits up to three or four since there is significant gain in the WSR rating for increasing from two to three snap-fits (68%) and from three to four snap-fits (32% additional). Adding these is useful when more resistance capability is desired and some redundancy is acceptable.

6 Conclusions

There is a need for a practical assembly constraint design tool to optimize the location, orientation, and quantity of assembly features that form a mechanical assembly configuration. By leveraging a previously developed constraint analysis technique, this paper provides a design optimization tool for mechanical part assemblies. The design tool and methodology are able to:

- Efficiently search the design space as constraint locations and orientations are modified both individually and simultaneously. Using a multidimensional search, superior constraint configurations can be synthesized.
- Evaluate the trade-off involved in selecting the optimal number of constraints. When constraint reduction is the objective, the best candidate for constraint removal can be identified to reduce redundancy while achieving a minimal decrease in total assembly resistance. For constraint addition, improvements in assembly ratings can be observed as redundancy increases to identify the point of diminishing returns.

The optimization tool can also provide useful domain-specific knowledge to understand the behavior of assembly performance as constraint configurations are modified. Because many design decisions need to be made contextually, the designer must be involved in using the tool as an expert system to understand the implication of design modifications. This qualitative understanding of assembly design is as important as the quantitative results of the design tool.

The design tool developed in this paper can be used to further understand more complex assembly designs and the interaction effects between the design variables. One important advancement would be to incorporate constraint stiffness into the model so that it better represents the deformation that occurs in overconstrained assemblies. In addition, it is crucial to be able to implement the current algorithm using parallel computing tools because the computation time increases exponentially as the search space dimension is increased. The tool would also benefit from work to identify circumstances in which analytical techniques could result in a provable global optimum, either by simplifying part geometry or focusing exclusively on dominant constraints.

References

[1] Luscher, A., 1996, "Part Nesting as a Plastic Snap-Fit Attachment Strategy," ANTEC 1996 Society of Plastic Engineers Annual Technical Conference and Exhibit, Indianapolis, IN, SPE Press.
[2] De Meter, E. C., 1993, "Selection of Fixture Configuration for the Maximization of Mechanical Leverage," Proceedings of the 1993 ASME Winter Annual Meeting, New Orleans, LA, Vol. 64, pp. 491–506.
[3] Cai, W., Hu, S. J., and Yuan, J. X., 1997, "A Variational Method of Robust Fixture Configuration Design for 3-D Workpieces," ASME J. Manuf. Sci. Eng., **119**, pp. 593–602.
[4] Chou, Y.-C., Chandru, V., and Barash, M. M., 1989, "A Mathematical Approach to Automatic Configuration of Machining Fixtures: Analysis and Synthesis," Trans. ASME J. Eng. Ind., **111**(4), pp. 299–306.
[5] Lakshminarayana, K., 1978, "Mechanics of Form Closure," New York, ASME Paper No. 78-DET-32.
[6] Salisbury, J. K., and Roth, B., 1983, "Kinematic and Force Analysis of Articulated Mechanical Hands," J. Mech., Transm., Autom. Des., **105**(1), pp. 35–41.
[7] Kerr, J., and Roth, B., 1986, "Analysis of Multifingered Hands," Int. J. Rob. Res., **4**(4), pp. 3–17.
[8] Hirai, S., and Asada, H., 1993, "Kinematics and Statics of Manipulation Using the Theory of Polyhedral Convex Cones," Int. J. Rob. Res., **12**(5), pp. 434–447.
[9] Xiong, Y., Ding, H., and Wang, M., 2002, "Quantitative Analysis of Inner Force Distribution and Load Capacity of Grasps and Fixtures," ASME J. Manuf. Sci. Eng., **124**, pp. 444–455
[10] Marin, R. A., and Ferreira, P. M., 2001, "Kinematic Analysis and Synthesis of Deterministic 3-2-1 Locator Schemes for Machining Fixtures," ASME J. Manuf. Sci. Eng., **123**(4), pp. 708–719.
[11] Marin, R. A., and Ferreira, P. M., 2002, "Optimal Placement of Fixture Clamps: Minimizing the Maximum Clamping Forces," Trans. ASME J. Manuf. Sci. Eng., **124**(3), pp. 686–694.
[12] Marin, R. A., and Ferreira, P. M., 2002, "Optimal Placement of Fixture Clamps: Maintaining Form Closure and Independent Regions of Form Closure," Trans. ASME J. Manuf. Sci. Eng., **124**(3), pp. 676–685.
[13] Ding, D., Liu, Y. H., Wang, M., and Wang, S., 2001, "Automatic Selection of Fixturing Surfaces and Fixturing Points for Polyhedral Workpieces," IEEE Trans. Rob. Autom., **17**(6), pp. 833–841.
[14] Schimmels, J. M., and Peshkin, M. A., 1992, "Admittance Matrix Design for Force-Guided Assembly," IEEE Trans. Rob. Autom., **8**(2), pp. 213–227.
[15] Asada, H., and By, A. B., 1985, "Kinematic Analysis of Workpart Fixturing for Flexible Assembly With Automatically Reconfigurable Fixtures," IEEE J. Rob. Autom., **2**, pp. 86–94.
[16] Hunt, K. H., 1978, *Kinematic Geometry of Mechanisms*, Oxford University Press, New York, NY.
[17] Lee, J. D., Hu, S. J., and Ward, A. C., 1999, "Workspace Synthesis for Flexible Fixturing of Stampings," ASME J. Manuf. Sci. Eng., **121**(3), pp. 478–484.
[18] Lee, J. D., and Haynes, L. S., "Finite-Element Analysis of Flexible Fixturing System," Trans. ASME J. Eng. Ind., **109**(2), pp. 134–139.
[19] Menassa, R. J., and DeVries, W. R., 1988, "Optimization Methods Applied to Selecting Support Positions in Fixture Design," Proceedings of the USA-Japan Symposium on Flexible Automation—Crossing Bridges: Advances in Flexible Automation and Robotics, Minneapolis, MN.
[20] Gui, X. W., Fuh, J. Y. H., and Nee, A. Y. C., 1996, "Modeling of Frictional Elastic Fixture-Workpiece System for Improving Location Accuracy," IIE Trans., **28**(10), pp. 821–827.
[21] Slocum, A. H., 1992, *Precision Machine Design*, Prentice-Hall, New Jersey.
[22] Whitehead, T. N., 1954, *The Design and Use of Instruments and Accurate Mechanism*, Dover Press, New York.
[23] Blanding, D., 1999, *Exact Constraint: Machine Design Using Kinematic Principles*, ASME Press, New York.
[24] Kriegel, J. M., 1994, "Exact Constraint Design," ASME International M E Congress and Exhibition (Winter Annual Meeting), Paper No. 94-WA/DE-18.
[25] Downey, K., Parkinson, A., and Chase, K., 2003, "An Introduction to Smart Assemblies for Robust Design," Res. Eng. Des., **14**, pp. 236–246.
[26] Soderberg, R., Lindkvist, L., and Dahlstrom, S., 2006, "Computer-Aided Robustness Analysis for Compliant Assemblies," J. Eng. Des., **17**(5), pp. 411–428.

[27] Whitney, D., 2000, *Mechanical Assemblies*, Oxford University Press, New York, NY.
[28] Whitney, D., Mantripragada, R., Adams, J. D., Rhee, S. J., 1999, "Designing Assemblies," Res. Eng. Des., **11**, pp. 229–253.
[29] Mantripragada, R., and Whitney, D. E., 1998, "The Datum Flow Chain: A Systematic Approach to Assembly Design and Modeling," Res. Eng. Des., **10**, pp. 150–165.
[30] Adams, J. D., Gerbino, S., Whitney, and Daniel, E., 1999, "Application of Screw Theory to Motion Analysis of Assemblies of Rigid Parts," Proceedings of the IEEE International Symposium on Assembly and Task Planning, Porto, Portugal, pp. 75–80.
[31] Adams, J. D., and Whitney, D. E., "Application of Screw Theory to Constraint Analysis of Assemblies of Rigid Parts," Proceedings of the IEEE International Symposium on Assembly and Task Planning, Porto, Portugal, pp. 69–74.
[32] Rusli, L., Luscher, A., and Schmiedeler, J., 2012, "Analysis of Constraint Configurations in Mechanical Assembly via Screw Theory," ASME J. Mech. Des, **134**(2), p. 021006.